

**PREPARATION AND CHARACTERISATION OF
STARCH PROPIONATE: EFFECT OF pH, NaCl
SALT SOLUTIONS AND APPLICATION AS
EMULSION STABILISER IN FOOD**

HONG LEE FEN

**UNIVERSITI SAINS MALAYSIA
2019**

**PREPARATION AND CHARACTERISATION OF
STARCH PROPIONATE: EFFECT OF pH, NaCl
SALT SOLUTIONS AND APPLICATION AS
EMULSION STABILISER IN FOOD**

by

HONG LEE FEN

**Thesis submitted in fulfillment of the requirements
for the degree of
Doctor of Philosophy**

June 2019

ACKNOWLEDGEMENT

Firstly, I would like to express my deep sense of gratitude to my main supervisor, Professor Dr. Peh Kok Khiang for his priceless supervision, knowledge, patience and motivation throughout the duration of my research project. I feel privileged to work with him as he always steers me in the right direction. He has taught me important skills especially on critical thinking and analytical skills, which I am truly grateful.

My sincere thanks also go to my co-supervisor, Associate Professor Dr. Cheng Lai Hoong and Dr. Lee Chong Yew. Whenever I felt of giving up, they would be there to give me strength to move on. I appreciated the advice, guidance and effort that they offered to me during my study.

Not forgetting, I am also thankful to Universiti Sains Malaysia for providing Postgraduate Research Grant Scheme (1001/PFARMASI/846066) and USM Fellowship to support my research project and lighten my financial burden.

I would like to acknowledge the laboratory assistants in School of Pharmaceutical Sciences and School of Industrial Technology, for their assistance at different phases of my research study.

I have been blessed with a group of cheerful and friendly colleagues, Dr. Tan Thuan Chew, Associate Professor Dr. Gan Chee Yuen, Dr. Kuan Yau Hong, Dr. Leong Yin Hui, Poh Lee Shang, Seow Eng Keng, Tan Hui Ling, Tan Chek Chuan, Muhammad Ezzuddin bin Ramli, Emily Wong Yii Ling, Khoo Pey Fang, Gabriel Loh Onn Kit,

Yong Hui Yin, Syuzeliana binti Shaari, Siti Rashima Romli, Dayang Norlaila Haji Latip, who continuously extending their helping hands and providing moral support to me during my PhD study.

Last but not the least, I dedicate my utmost gratitude and appreciation to my beloved family members. I will forever remember their wise counsel and appreciate them for lending a sympathetic ear whenever I need them. It is quite impossible for me to complete this research project without their constant support and encouragement.

TABLE OF CONTENTS

ACKNOWLEDGEMENT	ii
TABLE OF CONTENTS	iv
LIST OF TABLES	xiv
LIST OF FIGURES	xvii
LIST OF SYMBOLS AND ABBREVIATIONS	xxiii
ABSTRAK	xxvi
ABSTRACT	xxviii
CHAPTER 1 – INTRODUCTION	1
1.1 Background	1
1.2 Problem statement	3
1.3 Aims and objectives for research	4
CHAPTER 2 – LITERATURE REVIEW	6
2.1 Overview of corn plant (<i>Zea mays</i>)	6
2.2 Molecular structure of starch granules	6
2.2.1 Amylose	9
2.2.2 Amylopectin	10

2.3	Starch crystal model	11
2.4	X-ray diffraction pattern	12
2.5	Pasting properties	13
2.6	Retrogradation and syneresis of starch	15
2.7	Swelling and solubility of starch	17
2.8	Effect of pH and NaCl salt on the properties of starch	18
2.9	Chemical modification on starch through esterification	20
2.10	Applications of starch ester	22
2.11	Formation of emulsion	26
	2.11.1 Emulsion instability	26
	2.11.2 Mechanism of destabilisation of emulsion during freeze-thaw cycle	28
	2.11.3 Emulsifier and stabiliser	30
2.12	Rheology	34
	2.12.1 Relationship between shear stress and shear rate	34
	2.12.2 Types of fluid flow	35
	2.12.3 Linear viscoelastic properties	38
2.13	Beta-carotene	39

CHAPTER 3 – PREPARATION AND CHARACTERISATION OF	41
PHYSICOCHEMICAL PROPERTIES OF	
STARCH PROPIONATE AND APPLICATION AS	
STABILISER	
3.1 Introduction	41
3.2 Materials and methods	42
3.2.1 Materials	42
3.2.2 Determination of amylose and amylopectin content	43
3.2.3 Preparation of starch propionate using alkaline catalyst	43
3.2.4 Determination of degree of substitution	45
3.2.5 Fourier transform infrared spectroscopy	46
3.2.6 Nuclear magnetic resonance	46
3.2.7 Powder diffraction	47
3.2.8 Measurement of contact angle	47
3.2.9 Swelling power and percentage of leaching	47
3.2.10 Preparation of oil-in-water emulsions	48
3.2.11 Centrifugation stress study	48
3.2.12 Measurement of emulsion viscosity	49
3.2.13 Statistical analysis	49

3.3	Results and discussion	49
3.3.1	Determination of amylose and amylopectin content	49
3.3.2	Effect of reaction time and mole ratio of starch to propionic anhydride on degree of substitution of starch propionate	49
3.3.3	Fourier transform infrared spectroscopy of native corn starch and starch propionate	52
3.3.4	Nuclear magnetic resonance spectroscopy of native corn starch and starch propionate	54
3.3.5	Crystalline patterns of native corn starch and starch propionate	56
3.3.6	Effect of propionylation on hydrophobicity of starch	57
3.3.7	Effect of propionylation on the swelling and leaching behaviour of starch	59
3.3.8	Physical stability of emulsions with starch propionate	64
3.3.9	Viscosity of emulsions with starch propionate	66
3.4	Conclusions	70
	CHAPTER 4 – DETERMINATION OF PHYSICAL PROPERTIES OF STARCH PROPIONATE (DEGREE OF SUBSTITUTION 0.21, REACTION TIME 1 h) IN DISTILLED WATER, DIFFERENT pH VALUES AND SODIUM CHLORIDE SALT SOLUTIONS	71
4.1	Introduction	71
4.2	Materials and methods	74

4.2.1	Materials	74
4.2.2	Preparation of starch propionate (DS 0.21, RT 1 h)	74
4.2.3	Preparation of phosphate buffer solutions at different pH values	75
4.2.4	Determination of physical properties of starch propionate (DS 0.21)	75
4.2.4(a)	Determination of pasting properties	75
4.2.4(b)	Determination of swelling power and percentage of leaching	75
4.2.4(c)	Determination of textural properties	76
4.2.4(d)	Determination of freeze-thaw stability	77
4.2.4(e)	Determination of interfacial tension	77
4.2.5	Statistical analysis	78
4.3	Results and discussion	78
4.3.1	Determination of pasting properties	78
4.3.1(a)	Effect of pH	79
4.3.1(b)	Effect of NaCl	84
4.3.2	Determination of swelling power and solubility	87
4.3.2(a)	Effect of pH	87

4.3.2(b) Effect of NaCl	88
4.3.3 Determination of textural properties	89
4.3.3(a) Effect of pH	90
4.3.3(b) Effect of NaCl	93
4.3.4 Determination of freeze-thaw stability	94
4.3.4(a) Effect of pH	94
4.3.4(b) Effect of NaCl	95
4.3.5 Determination of interfacial tension	96
4.3.5(a) Effect of pH	96
4.3.5(b) Effect of NaCl	98
4.3.6 Physical properties of starch propionate	99
4.4 Conclusions	99
CHAPTER 5 – EVALUATION OF STARCH PROPIONATE AS EMULSION STABILISER IN COMPARISON WITH OCTENYLSUCCINATE STARCH	100
5.1 Introduction	100
5.2 Materials and methods	101
5.2.1 Materials	101

5.2.2	Preparation of starch propionate	101
5.2.3	Determination of degree of substitution	101
5.2.4	Determination of intrinsic viscosity and molecular mass	102
5.2.5	Preparation of oil-in-water (O/W) emulsions	103
5.2.6	Rheological properties	104
5.2.7	Determination of Sauter mean droplet diameter	104
5.2.8	Determination of creaming index and storage study	105
5.2.9	Statistical analysis	105
5.3	Results and discussion	106
5.3.1	Determination of degree of substitution, intrinsic viscosity and molecular mass	106
5.3.2	Rheological properties	107
5.3.3	Particle size determination	115
5.3.4	Creaming index and storage study	117
5.4	Conclusions	119
CHAPTER 6 – EFFECT OF pH AND SALT ON FREEZE-THAW CYCLE STABILITY OF STARCH PROPIONATE EMULSION AND BETA-CAROTENE BIOACCESSIBILITY		120
6.1	Introduction	120

6.2	Materials and methods	122
6.2.1	Materials	122
6.2.2	Preparation of starch propionate	122
6.2.3	Preparation of phosphate buffer solutions of different pH values	122
6.2.4	Preparation of beta-carotene emulsion	122
6.2.5	Rheological properties of emulsion	123
6.2.6	Freeze-thaw cycle stability of emulsion	123
6.2.6(a)	Determination of Sauter mean droplet diameter	123
6.2.6(b)	Microstructure of emulsion	123
6.2.6(c)	Stability determination of emulsion	124
6.2.7	Determination of free fatty acid released and beta-carotene bioaccessibility	124
6.2.7(a)	Oral phase	124
6.2.7(b)	Gastric phase	125
6.2.7(c)	Small intestinal phase	125
6.2.7(d)	Determination of free fatty acid released	126
6.2.7(e)	Assessment of beta-carotene bioaccessibility	128

6.2.8	Statistical analysis	129
6.3	Results and discussion	129
6.3.1	Determination of rheological property of emulsion	129
6.3.1(a)	Effect of pH	129
6.3.1(b)	Effect of NaCl	132
6.3.2	Sauter mean droplet diameter, microstructure and stability of emulsion	133
6.3.2(a)	Effect of pH	133
6.3.2(b)	Effect of NaCl	143
6.3.3	Determination of free fatty acid released	150
6.3.3(a)	Effect of pH	151
6.3.3(b)	Effect of NaCl	153
6.3.4	Beta-carotene bioaccessibility	156
6.3.4(a)	Effect of pH	157
6.3.4(b)	Effect of NaCl	158
6.4	Conclusions	160

CHAPTER 7 – GENERAL CONCLUSIONS	161
CHAPTER 8 – RECOMMENDATION FOR FUTURE STUDIES	165
8.1 Preparation of nanosized starch propionate for development of Pickering emulsion	165
8.2 Shelf-life determination of starch propionate (DS 0.21, RT 1 h)	165
8.3 Effect of other factors on physical properties of starch propionate	166
8.4 Application of starch propionate (DS 0.21, RT 1 h) in products	166
REFERENCES	167
APPENDICES	
LIST OF PUBLICATIONS	

LIST OF TABLES

		Page
Table 2.1	Properties of different starch from various sources (Li, 2014).	7
Table 2.2	Comparison of structural and physical properties of amylose and amylopectin (Li, 2014).	9
Table 2.3	Degree of substitution for METHOCEL products (Dow Chemical Company, 2002).	31
Table 3.1	Reaction parameters for the preparation of starch propionates.	44
Table 3.2	Contact angle (θ) values of the prepared various starch propionates. Mean \pm standard deviation, N = 6.	59
Table 3.3	Swelling power and percentage of leaching of native corn starch and various starch propionates at incubation temperature of 40 °C. Mean \pm standard deviation, N = 3.	61
Table 3.4	Swelling power and percentage of leaching of native corn starch and various starch propionates at incubation temperature of 90 °C. Mean \pm standard deviation, N = 3.	63
Table 3.5	Viscosities of oil-in-water emulsions prepared with 15% (w/w) of starch propionate. Mean \pm standard deviation, N = 3.	67
Table 3.6	Viscosities of oil-in-water emulsions prepared with 20% (w/w) of starch propionate. Mean \pm standard deviation, N = 3.	68
Table 3.7	Viscosities of oil-in-water emulsions prepared with 25% (w/w) of starch propionate. Mean \pm standard deviation, N = 3.	69

Table 4.1	Pasting parameters of starch propionate in distilled water and buffer solutions at different pH values. Mean \pm standard deviation, N = 3.	80
Table 4.2	Pasting parameters of starch propionate in distilled water and various concentrations of salt solutions. Mean \pm standard deviation, N = 3.	86
Table 4.3	Swelling power and percentage of leaching of starch propionate in distilled water and buffer solutions at different pH values. Mean \pm standard deviation, N = 3.	88
Table 4.4	Swelling power and percentage of leaching values of starch propionate in distilled water and various concentrations of salt solutions. Mean \pm standard deviation, N = 3.	89
Table 4.5	Textural parameters of starch propionate in distilled water and buffer solutions at different pH values. Mean \pm standard deviation, N = 10.	92
Table 4.6	Textural parameters of starch propionate in distilled water and various concentrations of salt solutions. Mean \pm SD, N = 10.	93
Table 4.7	Physical properties of starch propionate.	99
Table 5.1	Sample codes for emulsions prepared with various concentrations of SP, OSA and olive oil.	103
Table 5.2	Degree of substitution (DS) and intrinsic viscosity $[\eta]$ of SP and OSA starch. Mean \pm standard deviation, N = 3.	106
Table 5.3	The flow parameters of emulsions stabilised by various concentrations of SP and OSA at 35 and 45% (w/w) of olive oil content. Mean \pm standard deviation, N = 3.	110
Table 6.1	Chemical composition of artificial saliva.	125

Table 6.2	The flow parameters of emulsions stabilised by starch propionate in distilled water and buffer solutions at different pH values. Mean \pm standard deviation, N = 3.	131
Table 6.3	The flow parameters of emulsions stabilised by starch propionate in distilled water and different concentrations of NaCl solutions. Mean \pm standard deviation, N = 3.	133

LIST OF FIGURES

		Page
Figure 2.1	Structure of starch molecules: (a) amylose and (b) amylopectin (Li, 2014).	8
Figure 2.2	Amylose is composed of left handed helix conformation containing six glucose units per turn (Cornell, 2004).	10
Figure 2.3	A cluster model of amylopectin with A, and B1-B3 chains. The chain carrying the reducing end (ϕ) is the C chain (Hizukuri 1986).	11
Figure 2.4	Starch granule is proposed to consist of amorphous and crystalline regions: (A) Microcrystalline lamellae stacks are separated by amorphous rings. (B) Enlarged view of the amorphous and crystalline regions. (C) Side chains of amylopectin are intertwined into double helices, producing crystalline lamellae while branching points are organised within the amorphous regions (Donald <i>et al.</i> , 1997).	12
Figure 2.5	(a) A-type and (b) B-type crystalline structures of amylose (Imberty <i>et al.</i> , 1991).	13
Figure 2.6	Pasting profile of starch (Dar, 2014).	14
Figure 2.7	Association of amylose strands during retrogradation (Haralampu, 2000).	16
Figure 2.8	Relationship between swelling power and water solubility index of rice starches (Kong <i>et al.</i> , 2015).	17
Figure 2.9	Chemical reaction between starch with (a) propionic anhydride and (b) vinyl propionate in the presence of sodium hydroxide as catalyst.	20
Figure 2.10	Emulsion is a thermodynamically unstable system (McClements, 2008).	26

Figure 2.11	Emulsion may experience different breakdown processes (Tadros, 2016).	28
Figure 2.12	Optical micrograph of emulsion (a) before freezing, (b) water formed ice and oil droplets formed solid crystal (c) ice melted but oil droplets remained solid and (d) fat melted. Polarised light was used to indicate oil droplets in crystalline form in (b), (c) and (d). Scale bar is 20 μm (Ghosh & Coupland, 2008).	29
Figure 2.13	Phenomenon of partial coalescence (Degner <i>et al.</i> , 2014).	29
Figure 2.14	Structures of (a) OSA starch (Simsek <i>et al.</i> , 2015) and (b) xanthan gum (Kumar <i>et al.</i> , 2018).	33
Figure 2.15	Shear flow of two adjacent plates (Zhong & Daubert, 2013).	34
Figure 2.16	Shear strain on cube (Nielsen, 2017).	34
Figure 2.17	Rheogram showing Newtonian and non-Newtonian fluids (Rao, 2007).	37
Figure 3.1	Chemical reaction during preparation of starch propionate.	45
Figure 3.2	Degree of substitution (DS) of various starch propionates (SP) prepared over a period of 12 h at starch: propionic anhydride mole ratio: (\square) 1:6, (\blacksquare) 1:4, (\blacksquare) 1:3.	50
Figure 3.3	FTIR spectra of (a) native corn starch and starch propionates 1:6 (1 h), 1:6 (6 h), 1:6 (12 h) and (b) native corn starch and starch propionates 1:3 (1 h), 1:4 (1 h), 1:6 (1 h).	52
Figure 3.4	^1H NMR spectra of (a) native corn starch and (b) starch propionate prepared with 1:6 mole ratio of starch to propionic anhydride and reaction time of 12 h (DS 0.94).	54

Figure 3.5	COSY spectrum of starch propionate prepared with 1:6 mole ratio of starch to propionic anhydride and reaction time of 12 h (DS 0.94).	56
Figure 3.6	X-ray patterns of (a) native corn starch and starch propionates 1:6 (1 h), 1:6 (6 h), 1:6 (12 h) and (b) native corn starch and starch propionates 1:3 (1 h), 1:4 (1 h), 1:6 (1 h).	57
Figure 3.7	Emulsion stability (ES) of oil-in-water emulsions prepared with 15% (w/w) of starch propionate obtained throughout reaction time of 12 h for starch: propionic anhydride at mole ratios of: (□) 1:6, (■) 1:4.	64
Figure 3.8	Emulsion stability (ES) of oil-in-water emulsions prepared with 20% (w/w) of starch propionates obtained with reaction time from 1 to 12 h for starch: propionic anhydride at mole ratios of: (□) 1:6, (■) 1:4, (■) 1:3.	65
Figure 3.9	Emulsion stability (ES) of oil-in-water emulsions prepared with 25% (w/w) of starch propionates obtained with reaction time from 1 to 12 h for starch: propionic anhydride at mole ratios of: (■) 1:6, (■) 1:4, (□) 1:3.	66
Figure 4.1	Dissociation of hydroxyk groups from starch in water.	72
Figure 4.2	The typical pasting profile of starch displaying the main pasting parameters (Food Network Solution, 2008).	79
Figure 4.3	Texture profile analysis (TPA) curve showing hardness and area under curve (Nishinari <i>et al.</i> , 2013).	90
Figure 4.4	Syneresis of starch propionate gel in pH 2.0.	95
Figure 4.5	Syneresis of starch propionate gel in: (✕) 1.0 M and (⊖) 2.0 M salt solutions.	96
Figure 4.6	Interfacial tension of olive oil with distilled water or buffer solutions without (□) or with (■) the presence of starch propionate.	97

Figure 4.7	Interfacial tension of olive oil with distilled water or salt solutions without (□) or with (■) the presence starch propionate.	98
Figure 5.1	Relationship between shear stress (σ) and shear rate ($\dot{\gamma}$) of emulsions prepared with 12 to 16% (w/w) of starch: (a) SP and (b) OSA with 35 and 45% (w/w) of olive oil content. Starch content at 35% (w/w) of olive oil content: (◆) 12%, (●) 14%, (▲) 16%. Starch content at 45% of olive oil content: (+) 12%, (✕) 14%, (■) 16%.	108
Figure 5.2	Storage modulus (G') and loss modulus (G'') as a function of frequency (f) for emulsions incorporated with 12 to 16% (w/w) of starch: (a) SP with 35% (w/w) of olive oil content, (b) SP with 45% (w/w) of olive oil content, (c) OSA with 35% (w/w) of olive oil content and (d) OSA with 45% (w/w) of olive oil content. G' for different starch stabiliser contents: (✕) 12%, (▲) 14%, (●) 16%. G'' for different starch stabiliser contents: (+) 12%, (△) 14%, (○) 16%. The inset represents part of the curve when y-axis was set at 0-1.2 Pa.	113
Figure 5.3	Sauter mean droplet diameter (d_{32}) for emulsions incorporated with 12 to 16% (w/w) of starch at 35 and 45% (w/w) of oil content. Sauter mean droplet diameter for emulsions prepared with SP starch at different oil content: (□) 35%, (■) 45%. Sauter mean droplet diameter for emulsions prepared with OSA starch at different oil content: (▣) 35%, (■) 45%.	116
Figure 5.4	Creaming index (CI) for emulsions prepared with 12 to 16% (w/w) of OSA starch at 35% (w/w) of oil content over 14 days of storage duration. OSA starch content: (◆) 12%, (●) 14%, (▲) 16%.	118
Figure 6.1	The flow of the experimental setup.	127
Figure 6.2	Relationship between shear stress (σ) and shear rate ($\dot{\gamma}$) of the emulsions prepared in (△) distilled water and different pH values, (○) pH 2.0, (■) pH 3.5, (●) pH 7.0, (✕) pH 9.0 and (▲) pH 11.5.	130

Figure 6.3	Relationship between shear stress (σ) and shear rate ($\dot{\gamma}$) of the emulsions prepared in (Δ) distilled water and different concentrations of salt solutions: (\times) 0.5 M, (\square) 1.0 M and (\blacksquare) 2.0 M.	132
Figure 6.4	Effect of pH on Sauter mean droplet diameter (d_{32}) of emulsions prepared in (\square) distilled water and buffer solutions { (\blacksquare) pH 2.0, (\boxtimes) pH 3.5, (\blacksquare) pH 7.0, (\boxtimes) pH 9.0 and (\boxtimes) pH 11.5 } before and after freeze-thaw cycle.	134
Figure 6.5	Microstructure of emulsions prepared at 0 freeze-thaw cycle: (a) distilled water, (c) pH 2.0, (e) pH 3.5, (g) pH 7.0, (i) pH 9.0, (k) pH 11.5 and 5 th freeze-thaw cycle: (b) distilled water, (d) pH 2.0, (f) pH 3.5, (h) pH 7.0, (j) pH 9.0, (l) pH 11.5.	136
Figure 6.6	Effect of pH 2.0 on stability of emulsion before and after freeze-thaw cycle.	142
Figure 6.7	Effect of NaCl on Sauter mean droplet diameter (d_{32}) of emulsions prepared in (\square) distilled water and salt solutions { (\blacksquare) 0.5 M, (\blacksquare) 1.0 M and (\boxtimes) 2.0 M } before and after freeze-thaw cycle.	143
Figure 6.8	Microstructure of emulsions prepared at 0 freeze-thaw cycle: (a) distilled water, (c) 0.5 M NaCl, (e) 1.0 M NaCl, (g) 2.0 M NaCl and 5th freeze-thaw cycle: (b) distilled water, (d) 0.5 M NaCl, (f) 1.0 M NaCl, (h) 2.0 M NaCl.	145
Figure 6.9	Effect of NaCl on stability of emulsions prepared in (\square) distilled water and salt solutions { (\boxtimes) 0.5 M, (\blacksquare) 1.0 M and (\boxtimes) 2.0 M } before and after freeze-thaw cycle.	149
Figure 6.10	Mean free fatty acid release profiles of emulsions prepared in distilled water (\bullet) and buffer solutions at pH: (---) 2.0, (---) 3.5, (---) 7.0, (---) 9.0 and (---) 11.5. The inset represents part of the curve when y-axis was set at 65-100%.	151

Figure 6.11	Mean percentage of free fatty acid released from emulsion in distilled water and buffer solutions of different pH after 120 min of incubation time.	152
Figure 6.12	Mean free fatty acid release profiles of emulsions prepared in distilled water (●) and different concentrations of salt solutions: (⊖) 0.5 M NaCl, (■) 1.0 M NaCl and (⊞) 2.0 M NaCl.	154
Figure 6.13	Mean percentage of free fatty acid released from emulsions in distilled water and different concentrations of salt solutions after 120 min of incubation time.	155
Figure 6.14	Bioaccessibility (%) results of beta-carotene from emulsions prepared in distilled water and buffer solutions at different pH values after 120 min of incubation time.	157
Figure 6.15	Bioaccessibility (%) results of beta-carotene from emulsions prepared in distilled water and different salt concentrations after 120 min of incubation time.	159

LIST OF SYMBOLS AND ABBREVIATIONS

a	Mark's variation of Staudinger exponent
BD	Breakdown
c	Concentration
CaCl_2	Calcium chloride
$\text{C}_5\text{H}_3\text{N}_4\text{O}_3\text{Na}$	Uric acid sodium salt
$\text{C}_3\text{H}_5\text{O}_3\text{Na}$	Lactic acid sodium salt
CI	Creaming index
Cu-K α	Copper K-alpha radiation
d_{32}	Sauter mean droplet diameter
d_i	droplet diameter
DMSO	Dimethyl sulfoxide
d_n	average droplet diameter
DS	Degree of substitution
ES	Emulsion stability
FFA	Free fatty acid
FTIR	Fourier Transform Infrared
FV	Final viscosity
G'	Storage modulus
G''	Loss modulus
H	Height
HCl	Hydrochloric acid
H_2NCONH_2	Urea
K	Mark's variation of Staudinger constant
k'	Constant

$K_3C_6H_5O_7 \cdot H_2O$	Potassium citrate
KCl	Potassium chloride
K_H	Consistency index
KH_2PO_4	Potassium phosphate
M	Molecular mass
\bar{M}_w	Weight-average molecular weight
n	Flow behaviour index
NaCl	Sodium chloride
NaOH	Sodium hydroxide
NH_4NO_3	Ammonium nitrate
n_i	Number of droplets in each size class
NMR	Nuclear Magnetic Resonance
OSA	Octenylsuccinylated starch
O/W	Oil-in-water
PTemp	Pasting temperature
PTime	Peak time
PV	Peak viscosity
RT	Reaction time
RVA	Rapid visco analyser
SB	Setback
SCFA	Short chain fatty acid
SD	Standard deviation
SP	Starch propionate
t/t_0	Time ratio between sample and solvent
TV	Trough viscosity

u	Velocity
W/O	Water-in-oil
W/O/W	Water-in-oil-in-water
ΔL	Changes in length
Δt	Changes in time
$[\eta]$	Intrinsic viscosity
η_{rel}	Relative viscosity
$\dot{\gamma}$	Shear rate
σ	Shear stress
η_{sp}	Specific viscosity
σ^2	Standard deviation
θ	Theta
$\sum n_i$	Total number of droplets
η	Viscosity
σ_0	Yield stress

**PENYEDIAAN DAN PENCIRIAN KANJI PROPIONATE: PENGARUH pH,
LARUTAN GARAM NATRIUM KLORIDA DAN APLIKASI SEBAGAI
PENSTABIL EMULSI DALAM MAKANAN**

ABSTRAK

Kanji “octenylsuccinate” (kanji ubahsuai) adalah satu-satunya penstabil emulsi yang boleh didapati secara komersil dalam industri makanan. Oleh itu, tepat pada masanya untuk meneroka kanji ubahsuai lain sebagai penstabil emulsi. Kanji propionate (KP) telah dikaji sebagai kanji rintang tetapi tidak dikaji sebagai penstabil emulsi. Walau bagaimanapun, kaedah penyediaannya adalah rumit dan melibatkan pelbagai langkah, masa tindak balas yang panjang dan penggunaan pemangkin toksik. Objektif kajian ini adalah untuk menyediakan KP dengan langkah mudah iaitu melibatkan hanya satu langkah pemprosesan dan penggunaan pemangkin mesra alam, diikuti dengan penilaian sebagai penstabil emulsi. KP dengan darjah penggantian (DP) 0.21-0.94 telah berjaya disediakan dengan menggunakan kanji jagung: “propionic anhydride” pada nisbah mol 1: 3, 1: 4 dan 1: 6, dengan masa tindak balas dari 1 - 12 h . “Propionylation” telah disahkan dengan FTIR dan NMR. Apabila DP meningkat, KP menunjukkan pengurangan kristaliniti tetapi peningkatan sifat hidrofobik seperti yang digambarkan oleh keputusan pembelauan sinar-X dan darjah sentuhan, masing-masing. Emulsi minyak-dalam-air yang stabil terhadap tekanan dari pengemparan telah dihasilkan dari KP (DP 0.21-0.94) dan mempunyai viskositi antara 993.3-5413.3 mPa.s. KP (DP 0.21) yang dihasilkan dengan kanji jagung:”propionic anhydride” dalam nisbah mol 1:3 dan masa tindak balas 1 jam telah dipilih untuk kajian selanjutnya. KP yang disediakan dalam pH antara 3.5-11.5 atau 0.5 M larutan NaCl menunjukkan peningkatan dalam viskositi pempesan, kuasa

pengembangan, dan sifat tekstur apabila berbanding dengan KP yang disediakan pada pH 2.0; dalam 1.0 M atau 2.0 M larutan NaCl. KP mampu mengurangkan ketegangan “interfacial” antara minyak zaitun/ air suling, minyak zaitun/ larutan penampapan (pH 2.0-11.5) dan minyak zaitun/ larutan garam (0.5-2.0 M). Perbandingan telah dilaksanakan ke atas keupayaan KP (DP 0.21) dan kanji OSA (DP 0.03) dalam penstabilan emulsi. Emulsi yang disediakan dari KP mempunyai tekanan “yield”, kelikatan dan modulus penyimpanan yang lebih tinggi secara statistik apabila dibandingkan dengan emulsi yang disediakan daripada OSA. Purata Sauter diameter titisan menjadi semakin kecil apabila kepekatan kanji meningkat tetapi menjadi semakin besar apabila kepekatan minyak meningkat. Emulsi KP adalah stabil pada suhu bilik semasa kajian penyimpanan tetapi emulsi OSA adalah tidak stabil. Pengaruh pH dan kepekatan garam terhadap kestabilan kitaran beku-cair emulsi yang disediakan dengan KP telah disiasat. Emulsi KP yang disediakan pada pH 3.5-11.5 atau 0.5 M larutan garam adalah stabil terhadap lima kitaran beku-cair. KP tidak menjejaskan “bioaccessibility beta-carotene” dalam emulsi. Secara kesimpulannya, KP berpotensi untuk digunakan sebagai agen pemekat, pengemulsi dan pentekstur dalam produk makanan.

**PREPARATION AND CHARACTERISATION OF STARCH PROPIONATE:
EFFECT OF pH, NaCl SALT SOLUTIONS AND APPLICATION AS
EMULSION STABILISER IN FOOD**

ABSTRACT

Octenylsuccinylated starch (a modified starch) is the only commercially available emulsion stabiliser in food industry. Hence, it is timely to explore other modified starch as emulsion stabiliser. Starch propionate (SP) has been evaluated as resistant starch but not as emulsion stabiliser. However, its preparation was complicated involving multiple steps, long reaction time and use of toxic catalyst. The objective of the study was to prepare SP using a simple, one step process with environmentally friendly catalyst, followed by evaluation as emulsion stabiliser. SP with degree of substitution (DS) of 0.21-0.94 was successfully prepared using corn starch to propionic anhydride at mole ratios of 1:3, 1:4 and 1:6, with reaction time from 1 – 12 h. The propionylation was confirmed with FTIR and NMR. As DS increased, SP showed a decrease in crystallinity but an increase in hydrophobicity as reflected from X-ray diffraction and contact angle results, respectively. Oil-in-water emulsions prepared with starch propionate (DS 0.21-0.94) with viscosities between 993.3-5413.3 mPa.s were stable under centrifugation stress study. SP (DS 0.21) prepared with corn starch:propionic anhydride at mole ratio of 1:3 and reaction time of 1 h was chosen for further study. SP prepared in pH 3.5-11.5 or 0.5 M salt solutions showed increased pasting viscosity, swelling property and textural property, when compared to SP prepared in buffer pH 2.0; 1.0 M salt solution or 2.0 M salt solutions. SP was able to reduce the interfacial tension between olive oil/ distilled water, olive oil/ buffer solutions (pH 2.0-11.5) and olive oil/ salt solutions (0.5-2.0

M). The emulsion stabilising property of SP (DS 0.21) was compared with octenylsuccinylated starch (OSA, DS 0.03). SP emulsion exhibited a significantly higher yield stress, apparent viscosity, and storage modulus (G'). Sauter mean droplet diameter of oil droplets in emulsion decreased with starch concentration but increased with oil concentration. SP emulsion was stable but not OSA starch emulsion when stored at room temperature. The influence of pH and salt content on freeze-thaw cycle stability of oil-in-water emulsion stabilised with SP was investigated. SP emulsions prepared in pH 3.5-11.5 or 0.5 M salt solution were stable after undergoing five freeze-thaw cycles. Starch propionate did not adversely affect the bioaccessibility of beta-carotene incorporated in the emulsion. In conclusion, SP has the potential to be applied as viscosifying, emulsifying and texturing agent in food products.

CHAPTER 1

INTRODUCTION

1.1 Background

Among all the cereal crops, 94% of cereal consumption comes from corn, wheat and rice. Starch extracted from corn is used to produce various products such as bread, porridge, steamed products, beverages and snacks (Gwirtz & Garcia-Casal, 2014; Ranum *et al.*, 2014). Native starch normally does not swell at cold temperatures (Wang *et al.*, 2014) and is prone to retrogradation and syneresis (Degner *et al.*, 2014; Fu *et al.*, 2015). These imperfect properties of native starch could be resolved by using modified starch. Modified starch particularly after through esterification, had improved properties such as transparency, freeze-thaw stability or syneresis, water absorption or swelling power, pasting viscosity, and gelatinisation (Colussi *et al.*, 2015; Lin *et al.*, 2017a; Shah *et al.*, 2017; Zhu, 2017).

During formation of emulsion, biopolymer based stabiliser has to adsorb on the surface of oil droplets and form an interfacial membrane to avoid aggregation of oil droplets. Stabilisation of oil droplets involves various mechanisms namely, steric, electrostatic and hydration repulsion. Food biopolymers that are commonly used to emulsify or stabilise emulsion are modified starch, proteins and hydrocolloids. Modified starch also stabilises emulsion through enhancing viscosity or formation of gels (McClements, 2015).

Starch acetate, octenylsuccinylated (OSA) starch and starch propionate are popular starch esters used in the food industry. The differences in fatty acid chain length impart different properties in these starch esters.

Starch acetate which is currently available commercially has a DS of 0.1. It is normally used to improve the textural property of food (Semeijn & Buwalda, 2018; Sun *et al.*, 2016) but not as a stabiliser. In comparison to starch acetate (having 2-carbon fatty acid chains), octenylsuccinylated (OSA) starch (12-carbon fatty acid chain) could provide sufficient lipophilicity to stabilise emulsions even at DS of 0.03. Only OSA starch exhibits the ability to stabilise emulsion and to encapsulate active ingredients such as vitamins and flavours (Agama-Acevedo & Bello-Perez, 2017; Jin *et al.*, 2018). On the other hand, starch propionate was studied as resistant starch (Annison *et al.*, 2003). Starch propionate is categorised as a type 4 resistant starch (RS4). Human and animal studies showed that starch propionate with degree of substitution (DS) ≥ 0.16 could resist intestinal digestion (Annison *et al.*, 2003; Clarke *et al.*, 2007). Starch propionate was fermented in the large intestine of rats, producing a large pool of short chain fatty acids especially propionic acid (Annison *et al.*, 2003). Production of short chain fatty acids reduced the colonic pH, thereby encouraging the growth of probiotic bacteria (Arcila & Rose, 2015; Haenen *et al.*, 2013) and competed with pathogenic bacteria in colonising the intestinal mucosa (Bender, 2017). Animal studies showed that short chain fatty acids (SCFA) are particularly high in the proximal large colon but declined toward the distal colon (den Besten *et al.*, 2013). The availability of short chain fatty acids in specific regions of the large bowel may be critical for disease prevention. Annison *et al.* (2003) showed that

starch propionate could reach the distal colon and be fermented to release specific short chain fatty acids.

1.2 Problem statement

Food biopolymers are commonly used as emulsion stabilizers in the food industry. Octenylsuccinylated (OSA) starch and xanthan gum are two commonly used emulsion stabilizers. However, both have shortcomings. Dokić *et al.*, (2012) reported that OSA emulsion creamed even when OSA starch was used up to 16% w/w. OSA starch itself when used in products such as mayonnaise, could not provide sufficient viscosity to the product. Most often, viscosifying agent such as xanthan gum had to be added (Krstonošić *et al.*, 2015). Xanthan gum, an anionic polysaccharide, due to its negative charge, may react with protein emulsifier to form insoluble complex at low pH. As a result, desorption of protein from oil droplets causes phase separation of emulsion (Owens *et al.*, 2018; Qiu *et al.*, 2015). Similarly, the presence of salt such as NaCl or CaCl₂ could cause creaming of emulsion stabilised with xanthan gum. The instability was due to ion binding, electrostatic screening or partial desorption of anionic biopolymer from the droplet surface (Qiu *et al.*, 2015).

As there are only a few emulsion stabilizers available commercially and OSA starch is the only modified starch in the food industry, it is timely to explore other modified starch as emulsion stabilizer. Starch propionate (having 3-carbon fatty acid chains) has been studied as resistant starch but it has not been evaluated as emulsion stabiliser. However, the reported preparation method of starch propionate (SP) was complicated involving multiple processing steps, long reaction time and use of toxic catalyst. There was pre-activation of starch in pyridine for two hours under nitrogen

flush in reflux condenser followed by a long reaction time of 22 hours to prepare starch propionate with DS between 0.21-2.92, using starch:propionic anhydride mole ratio of 1:4 to 1:9 (Garg & Jana, 2011; Santayanon & Woothikanokkhan, 2003). Pyridine is a toxic compound and could cause environmental pollution. It may take several months or years to be broken down into other compounds when released into air (Public Health Statement, 1992). As such, esterification process that involves pyridine as catalyst has to be carried out in a special flask such as reflux condenser.

Hence, in the present study, starch propionate is prepared using a single step, simple and environmentally friendly method. The focus is on the characterisation of less studied moderately substituted starch propionate.

1.3 Aims and objectives of research

The objective of the present study was to prepare a modified starch having emulsion stabilizing property. Starch propionate was prepared using a single step, more simple processing method and environmentally friendly catalyst. Starch propionate with suitable degree of substitution was chosen for further study as emulsion stabiliser in food. The starch propionate was investigated at environments normally encountered by food such as pH and salt content. The experiments were carried out in different stages.

- 1) Preparation and characterisation of the physicochemical properties of starch propionate with different degrees of substitution and preliminary evaluation as emulsion stabiliser.
- 2) Determination of physical properties of starch propionate with suitable degree of substitution in distilled water, different pH values and salt solutions.

- 3) Evaluation of effectiveness of starch propionate as emulsion stabiliser in comparison with octenylsuccinylated (OSA) starch.
- 4) Study of the influence of pH and salt on freeze-thaw stability of starch propionate emulsion and beta-carotene bioaccessibility.

CHAPTER 2

LITERATURE REVIEW

2.1 Overview of corn plant (*Zea mays*)

Corn is one of the richest source of starch in the world. Originally, corn is native to North American continent. It has been consumed in both North and South America for thousands of years and spread to Europe and Asia approximately 500 years ago. Corn is a member of the grass family, called *Zea mays*. The plant is known as corn in United States and as maize in other parts of the world. Corn starch is normally extracted from its seed.

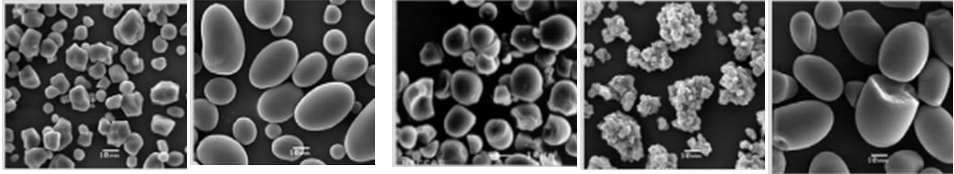
The processing of corn is known as corn wet milling and corn refining (Gwirtz & Garcia-Casal, 2014). In the food industry, corn starch is used to give texture to food. Corn starch is also processed into liquid glucose, dextrose monohydrate, dextrose anhydrous, sorbitol, yellow and white dextrin (NPCS Team, 2014). In the nonfood industry, corn starch is used in a broad range of industrial products such as paper, textiles and building materials (Kulshreshtha *et al.*, 2017; NPCS Team, 2014).

2.2 Molecular structure of starch granules

Li (2014) reported that starch granules obtained from different crops showed variation in size, shape, and amylose content (Table 2.1). Potato starch has large granule size while rice starch has the smallest granule size. Starch from different botanical sources also displays different amylose content. Starch granule itself could be used as a substrate in delivery systems or for stabilising emulsion. Quinoa starch

having a naturally fine structure (0.5–3 μm) could form Pickering emulsion in its granular structure (Marefati *et al.*, 2013). Porous starch granule produced as a result of enzyme hydrolysis was used to encapsulate olive oil or lipophilic drug (Lei *et al.*, 2018; Zhang *et al.*, 2013a).

Table 2.1 Properties of different starch from various sources (Li, 2014).

Source of Starch	Corn	Potato	Tapioca	Rice	Sago
Granule size (μm)	14	41	17	3	33
Amylose content (%)	25	20	17	19	28
Morphology (SEM)					

Starch is built up of six-carbon sugar D-glucose (Figure 2.1). There are two types of starch polymers, amylose and amylopectin (Figure 2.1). Amylose has a linear molecular structure consisting of predominantly α -(1,4) bonds. Amylose molecules are slightly branched. Amylopectin is a highly branched polymer with α -(1,6) bonds at branch points (Li, 2014).

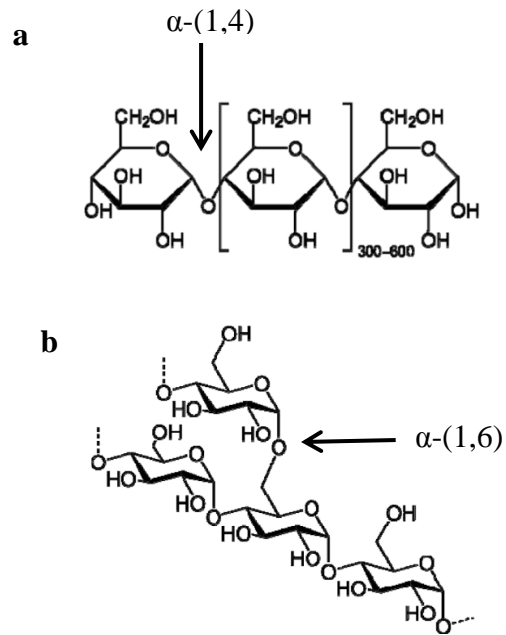


Figure 2.1 Structure of starch molecules: (a) amylose and (b) amylopectin (Li, 2014).

Although both polymers are composed of D-glucose, the structural differences between these two polymers contribute to a distinct variation in starch behaviours as shown in Table 2.2. Owing to the strong molecular interactions, amylose typically requires a very high temperature cook-up, and tends to retrograde forming gel and film. Amylopectin having branched structure has weaker intermolecular interactions due to steric hindrance. It forms a more stable solution (slower rate of retrogradation) and is suitable for high moisture applications. Owing to its larger size, amylopectin forms a more viscous solution, has a lower gelatinisation temperature and is easier to be used compared to amylose (Li, 2014).

Table 2.2 Comparison of structural and physical properties of amylose and amylopectin (Li, 2014).

Factor	Amylose	Amylopectin
Shape	Predominantly linear	Branched
Linkage	Primarily α -(1,4)	α -(1,4) and α -(1,6)
Molecular weight (Daltons)	< 1.5 million	50-500 million
Number of chains (branches) per molecule	1-10	200-750
Films	Strong	Weak
Gel formation	Strong	Weak
Iodine stain	Blue	Red-violet
Retrogradation	Fast	Slow

2.2.1 Amylose

Amylose is essentially a linear polymer composed almost entirely of α -(1,4) linked D-glucose. The weight-average molecular weight (\bar{M}_w) and degree of branching of amylose was reported as 1.8×10^7 to 4.8×10^7 g/mol (Syahariza *et al.*, 2013) and 0.2% (Sorndech *et al.*, 2016), respectively.

There are two typical properties of amylose, namely its behaviour to form complex with ligands and its tendency to aggregate in neutral aqueous solution. In neutral solutions, amylose exists as a random coil. However, in the presence of ligands, including iodine and alcohol, it will change its conformation from amylose double helices to a single helix. This would result in the formation of so called V-amylose that is compact and has a central hydrophobic cavity whereby ligands can reside (Dries *et al.*, 2016; Li, 2014). V-amylose has a helical structure with six D-glucose per helical turn. The interior of the helix is hydrophobic with a diameter of 0.6 nm, whereas the outer diameter of helix is 1.4 nm and a pitch per helical turn is 0.8 nm

(Figure 2.2) (Cornell, 2004). Iodine complexation has become an important diagnostic tool for the characterisation of starch amylose content (Kaufman *et al.*, 2015).

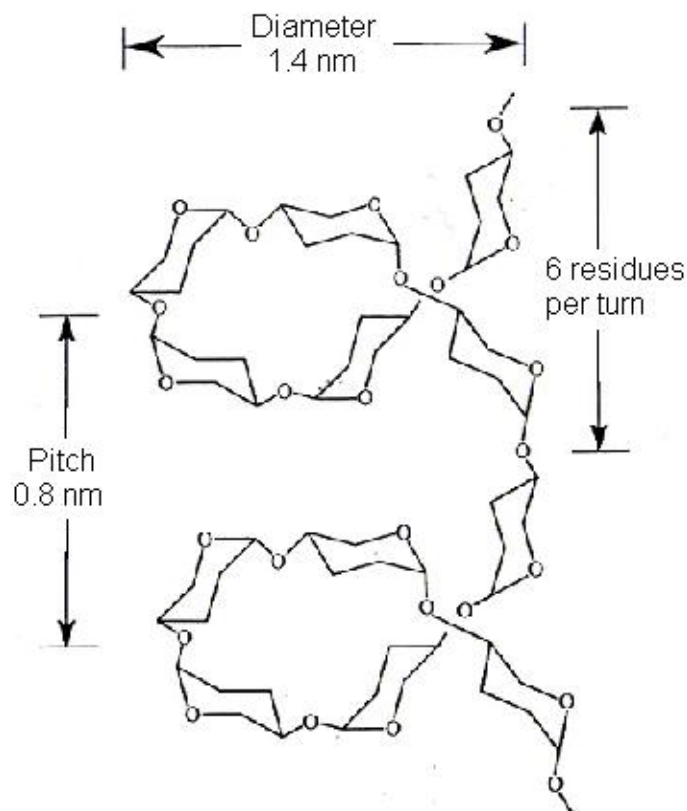


Figure 2.2 Amylose is composed of left handed helix conformation containing six glucose units per turn (Cornell, 2004).

2.2.2 Amylopectin

Amylopectin is the predominant molecule in most normal starches. It is a branched polymer. Amylopectin with weight-average molecular weight (\bar{M}_w) in the order of 5.9×10^7 to 8.2×10^8 g/mol is one of the largest known naturally occurring polymers (Kowittaya & Lumdubwong, 2014). The degree of branching for amylopectin has been reported as 3.5% (Sorndech *et al.*, 2016).

The amylopectin molecule consists of three groups of glucose chains, A, B and C chains. A-chains are unbranched and are linked to the molecule through their

reducing end-group; B chains are joined to the molecule in the same way but carry one or more A-chains; and C-chain, which carries the reducing end-group of the molecule (Figure 2.3).

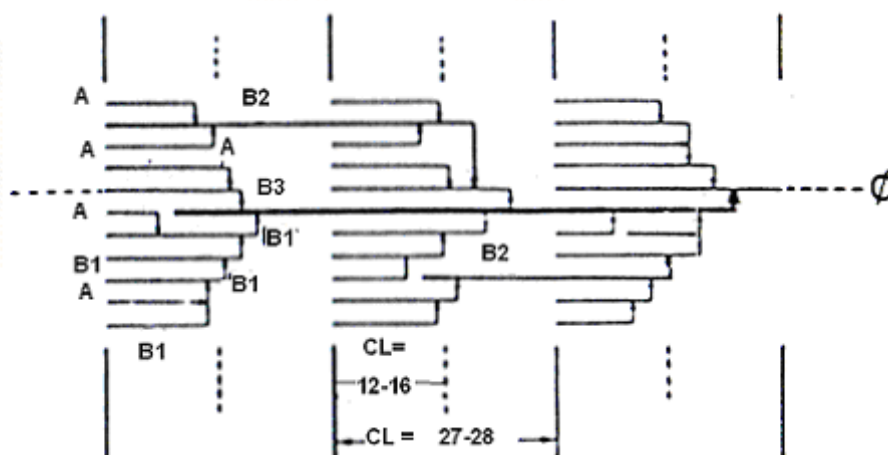


Figure 2.3 A cluster model of amylopectin with A, and B1-B3 chains. The chain carrying the reducing end (ϕ) is the C chain (Hizukuri 1986).

Kowittaya & Lumdubwong (2014) studied the branch chain profiles of amylopectin from different rice cultivars. They reported that mole fractions of A chain (degree of polymerisation of 6-12), B1 chain (degree of polymerisation 13-24), B2 chain (degree of polymerisation of 25-36) and B3 chain (degree of polymerisation ≥ 37) were 35.35-45.17%, 47.35-56.73%, 5.86-6.46% and 1.21-1.48%, respectively.

2.3 Starch crystal model

Small angle and wide angle X-ray scattering contribute to the 'lamellar stack' model (Figure 2.4) proposed by Donald *et al.* (1997). Starch granule contains alternating amorphous and crystalline lamellae, with a periodicity of ~ 9 nm as shown in Figure 2.4. Stacks of microcrystalline lamellae are separated by amorphous growth rings.

The double helices formed by adjacent chains of amylopectin give rise to crystalline lamellae. Branching points form the amorphous regions (Donald *et al.*, 1997).

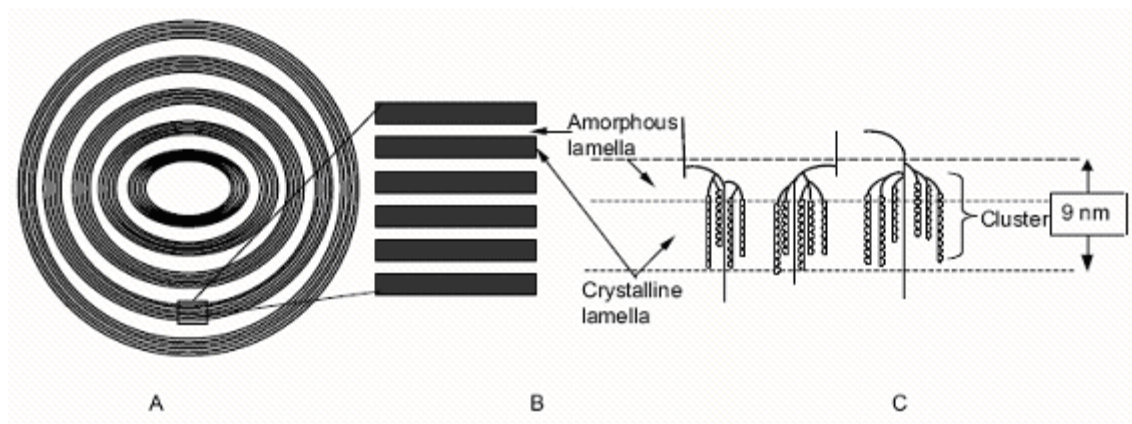


Figure 2.4 Starch granule is proposed to consist of amorphous and crystalline regions: (A) Microcrystalline lamellae stacks are separated by amorphous rings. (B) Enlarged view of the amorphous and crystalline regions. (C) Side chains of amylopectin are intertwined into double helices, producing crystalline lamellae while branching points are organised within the amorphous regions (Donald *et al.*, 1997).

2.4 X-ray diffraction pattern

When X-ray wave is directed into a crystal material, it splits to form a unique pattern of the crystal structure. This technique has been used to study starch's semicrystalline nature. Formation of crystallinity in starch is contributed by the external part of amylopectin chains, which interact with each other as well as with water molecules (Zhu, 2015). Figure 2.5 shows the common starch crystal model, A and B patterns. The A-type crystal pattern has eight water molecules per unit cell, while B-type crystal pattern consists of 36 water molecules. The A-type accommodates the double helices relatively more densely than the B-type crystal (Imberty *et al.*, 1991; Wu & Sarko, 1978).

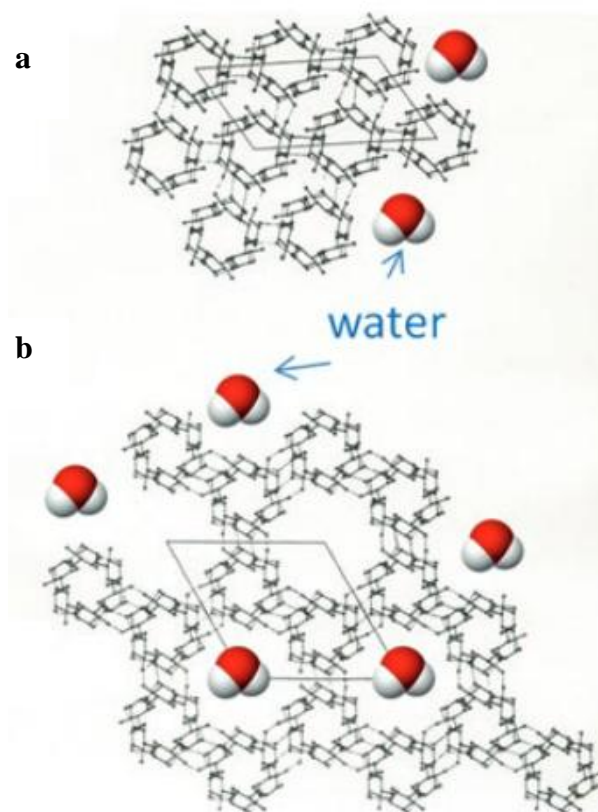


Figure 2.5 (a) A-type and (b) B-type crystalline structures of amylose (Imberty *et al.*, 1991).

2.5 Pasting properties

Pasting profiling is usually conducted with Rapid Visco Analyser (RVA) (Newport Scientific Pty. Ltd, Warriewood, NSW, Australia). RVA operates mixing, heating, and cooling in a controlled manner, thus producing highly reproducible pasting profiles. In industry, behaviour of different starches during pressure cooking process could be known through analysis using RVA. Figure 2.6 shows a series of granular changes during thermal and cooling profiling. As temperature increases, a rise in viscosity is due to swelling of starch granules. Amylose molecules begin to leach from the granules. Viscosity continues to increase as temperature increases until a peak viscosity is obtained. At this point, most granules are fully swollen. At the holding period of 95 °C, the granules start to break down followed by solubilisation

and aggregation of the starch polymer. At the same time, the spindle will start “cutting” through the paste. The effect of “cutting” causes a drop in viscosity. As temperature drops to 50 °C, amylose and amylopectin polymers present in the paste begin to reorganise leading to another rise in viscosity. This successive rise in viscosity is known as set-back (Dar, 2014).

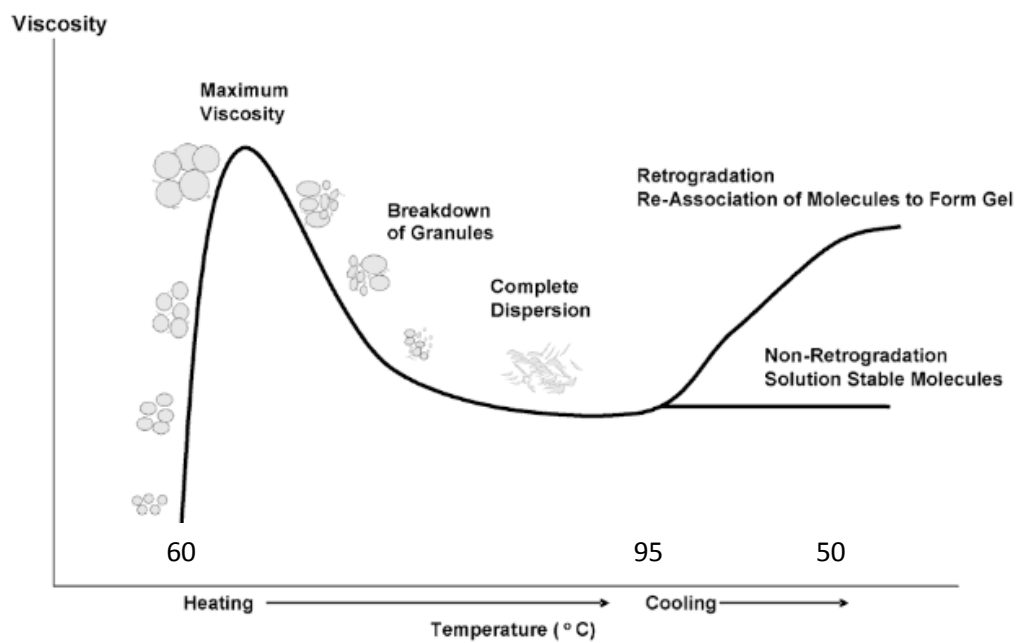


Figure 2.6 Pasting profile of starch (Dar, 2014).

RVA could be used to determine the quality of rice, quality of flour for cake making and used in simulation and monitoring of process (Martínez, 2019).

When rice is added as an ingredient to enhance the organoleptic properties of an end product, the property of rice has to be determined. There are different types of rice such as waxy rice (0-5% amylose), intermediate amylose rice (20-25%) and high amylose rice (25-33%). These grains exhibit different functional properties especially on the degree of retrogradation. Retrogradation is associated with the

degree of stickiness of cooked grains and is an important factor in the culinary quality (Martínez, 2019).

By using RVA, the apparent viscosity of the batter after mixing all the ingredients could serve as an interesting indicator related to the quality of a final product. Apparent viscosity has been related with the important features of cake, namely volume and texture. One of the most important parameters in flour during cake baking is the pasting temperature, whereby it has a strong influence on the expansion of air bubbles during the baking before the cake sets (Martínez, 2019).

The processing of food products usually involves various steps. The ability to control these steps is important for improving the quality of the end product and optimising the process efficiency by increasing the yield or reducing the costs. RVA offers an alternative testing which simulate the processes on a small scale. For instance, RVA was used to cook pudding mix and monitor its viscosity by measuring its pasting properties in the step process (Martínez, 2019).

2.6 Retrogradation and syneresis of starch

When gelatinised starch is cooled and stored, both the amylose and amylopectin molecules rearrange into a rigid or crystalline structure, which is known as retrogradation process. Miles *et al.* (1985) reported that retrogradation of starch took place in two stages. In the first stage, amylose gelation proceeded, resulting in rigidity of starch gels. In the second stage, thermo-reversible crystallisation of amylopectin took place causing a long-term increase in the elastic modulus of starch gels. The second stage happened at a slower rate and continued for a week at 26 °C

for 20% (w/v) of starch gel. A higher starch content and lower temperature stimulated the rate of retrogradation (Miles *et al.*, 1985; Wang *et al.*, 2015). The crystals of amylopectin dissociated at approximately 60 °C in most native starches (Fu *et al.*, 2015; Zhang *et al.*, 2014), while amylose crystallites dissociated at approximately 120 °C (Zhang *et al.*, 2013b).

Haralampu (2000) proposed that amylose crystal was formed through junction zones of amylose double helices. The individual strands in the helix consisted of six glucose units per turn. As retrogradation proceeded, the double helices pack densely forming crystalline region (Figure 2.7).

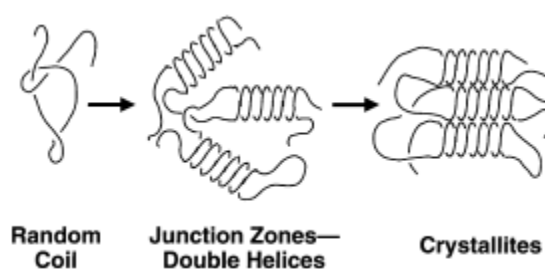


Figure 2.7 Association of amylose strands during retrogradation (Haralampu, 2000).

Junction zones are the regions composed of supramolecular bundles of polymer molecules. In a junction zone, the D-glucose units of two or more polysaccharide chains interacted through noncovalent bonds to form a microcrystalline structure (BeMiller, 2019).

Freeze-thaw cycles promoted the formation or expansion of junction zones to give rise to crystalline growth (Daniel & Whistler, 1985). The junction zones were produced through the association of starch molecules producing gel or cross-bonded

structure. Association of starch molecules led to excretion of water and this phenomenon was known as syneresis (Daniel & Whistler, 1985).

2.7 Swelling and solubility of starch

Heating of starch in the presence of large amount of water may cause melting of the crystalline structure within the granular structure of starch as water molecules interact with the hydroxyl groups of starch molecules through hydrogen bonding. Disruption of granular structure of starch led to an increase in starch swelling and α -glucan leaching (Wang *et al.*, 2014). Swelling power and solubility of starch were shown to be temperature dependent (Figure 2.8). The values of swelling power and solubility increased with an increase in temperature due to weakening of internal associative forces that maintained the granular structure (Kong *et al.* 2015).

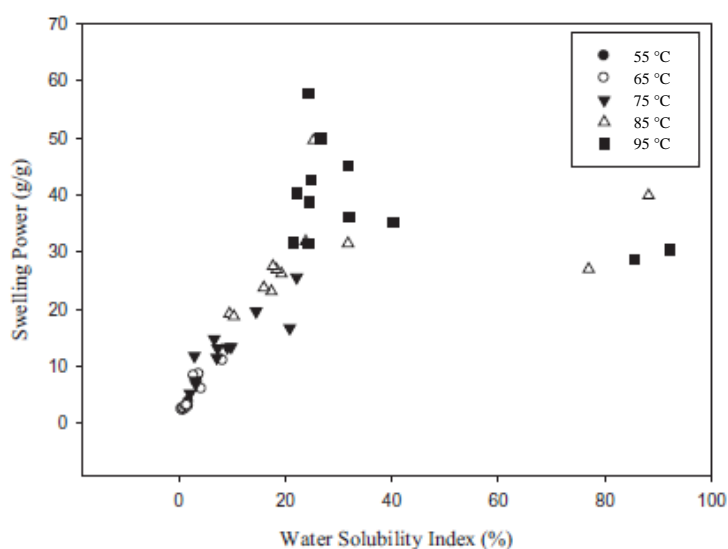


Figure 2.8 Relationship between swelling power and water solubility index of rice starches (Kong *et al.*, 2015).

Mir & Bosco (2014) showed that swelling power of starch was dependent on the ratio of amylose and amylopectin. They reported that Indian Himalayan rice variety Jehlum (amylose content of 32.76%) had the lowest swelling power of 10.56 g/g

while rice variety, Khosar (with the lowest amylose content of 22.69%) had the highest swelling power of 19.54 g/g. Lin *et al.* (2016) suggested that swelling of starch was predominantly attributed to amylopectin.

2.8 Effect of pH and NaCl salt on properties of starch

Acid hydrolysis was shown to increase the relative crystallinity of starch, by preferentially attacking the amorphous regions of starch granules (de la Concha *et al.*, 2018; Kim *et al.*, 2013). Hydrogen ions tend to attack α -(1,6) and α -(1,4) glycosidic bonds of starch. However, with prolonged hydrolysis time, acid would slowly enter and degrade the crystalline domains (Wang & Copeland, 2015; Xia *et al.*, 2017). In the early phase of acid treatment, hydrogen ions tend to hydrolyse amylose chains to a greater extent than amylopectin (Jiang *et al.*, 2018; Shi *et al.*, 2016a). When starch was hydrolysed with 2.2 N HCl at 35 °C for 40 days, the molecular weight of starch polymers in yellow, red and purple potato starch dropped from 4.279×10^6 - 4.279×10^7 to 3.717×10^3 - 5.196×10^3 g/mol. After acid hydrolysis, starch granules were damaged while some granules had lost their birefringence (Yang *et al.*, 2018). Birefringence is a unique feature in native starch whereby it has the ability to doubly refract polarized light. Native starch could exhibit birefringence because starch molecules are radially arranged within its granular structure. When the crystalline organisation within the starch granule is disrupted or destroyed, starch will lose its birefringence (Alcázar-Alay & Meireles, 2015). In another study, waxy starch was hydrolysed with 2 M HCl at 20 °C for 12 days. Amylose was hydrolysed first, followed by long amylopectin branches, B2 and B3 chains (Chen *et al.*, 2017).

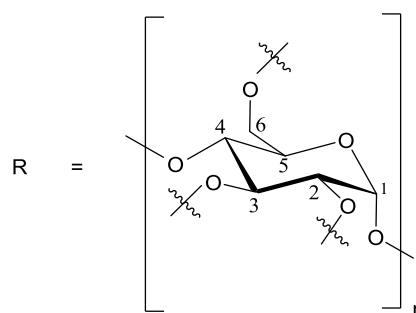
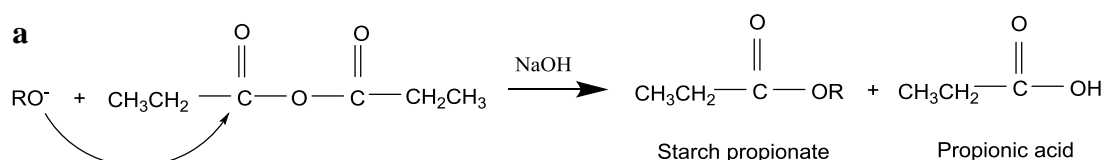
At equilibrium, starch has negative a charge (due to the dissociation of hydrogen ion from hydroxyl group of starch) while water has a positive charge. In the presence of sodium hydroxide, sodium cation enters the starch granules because its concentration in starch granules is low. At the same time, hydrogen ions from starch granules leave the starch granules. This situation occurs because of the concentration gradient for both cations. Inside starch granules, the alcohol group that has been replaced with sodium ion is changed to salt form. This salt form dissociates much easily compared to the hydrogen form, thus increasing the Donnan potential. As a result, anions from sodium hydroxide are expelled at ease (Oosten, 1982). Oosten (1990) reported that anions are the actual cause for gelatinising starch while cations protect the granular structure from gelatinisation. If sodium hydroxide is added continuously, gelatinisation will occur because hydroxyl groups (anions) preferentially enter starch granules and disrupt the hydrogen bonds. This is because the penetration of anions overrides the repulsion force of Donnan potential (Oosten, 1982).

Qiao *et al.* (2016) reported that alkali treated regular maize starch increased the thickness of the granule's crystalline lamellae (caused by swelling effect from alkali) but reduced thickness of the granule's amorphous lamellae (caused by leaching out of starch molecules). In high amylose maize starch, alkali treatment was found to increase both the amorphous and crystalline lamellae due to swelling effect. When the rate of digestion was compared between both alkali treated starches, regular maize starch appeared to have higher digestion rate than high amylose maize starch. This was due to the presence of pores in the regular maize starch granule and short double helices (due to the short side chains) causing "weak points" in the crystalline region.

The effect of salt was similar to the effect of sodium hydroxide whereby anions caused gelatinisation of starch while cations protected starch by preventing it from gelatinisation (Oosten, 1982).

2.9 Chemical modification on starch through esterification

Starch ester is usually prepared through chemical reaction between starch and acid anhydride or vinyl ester (Figure 2.9). The reactions proceed according to nucleophilic substitution at the unsaturated carbon producing starch acetate. Sodium hydroxide (NaOH) acts as a promotor (Shrestha & Halley, 2014). The hydroxyl groups on C₆ of the starch molecule is said to be more reactive than C₂ and C₃ due to steric hindrance. C₆ is located at the exterior surface of the starch molecule, thus it easily takes place in chemical reactions. Between C₂ and C₃, C₂ is more reactive because it is positioned closer to the hemi-acetal of the starch molecule and is thus more acidic than C₃ (Khlestkin *et al.*, 2018; Shrestha & Halley, 2014).



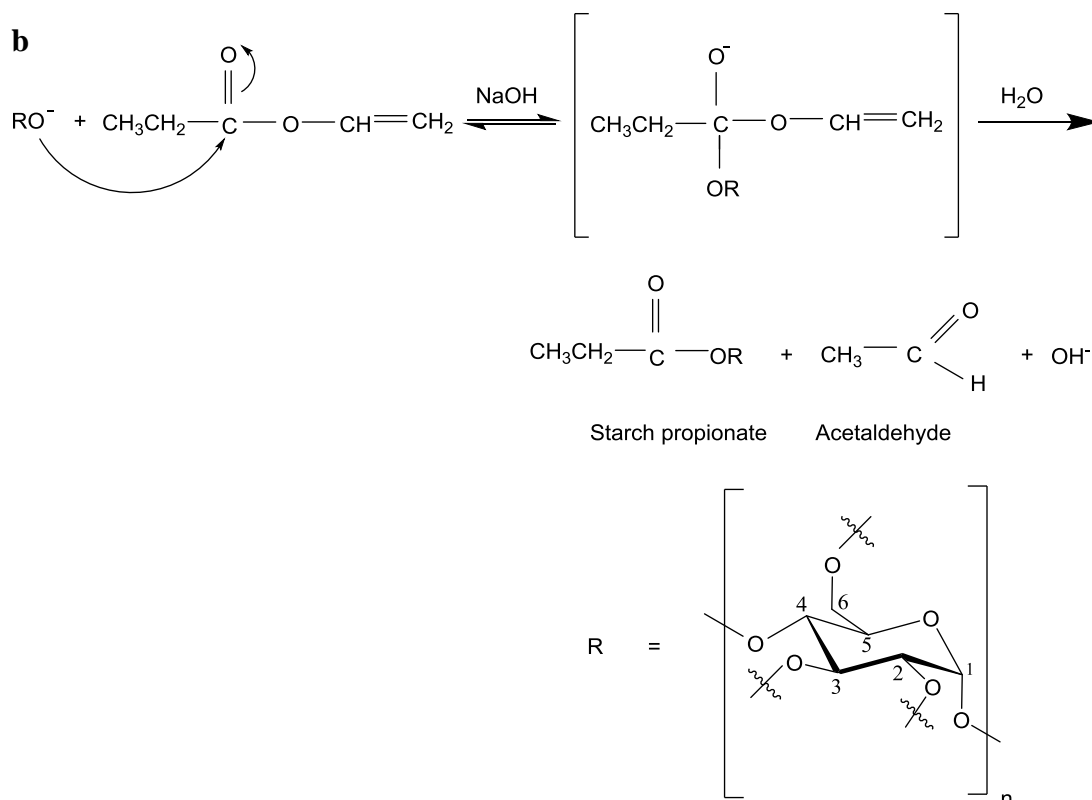


Figure 2.9 Chemical reaction between starch with (a) propionic anhydride and (b) vinyl propionate in the presence of sodium hydroxide as catalyst.

Different types of catalysts have been reported during esterification of starch namely, acid, sodium hydroxide, pyridine, ionic liquid and enzyme. Tupa *et al.* (2018) conducted esterification using L-tartaric acid as catalyst and reaction temperature of 130 °C to produce starch propionate with degree of substitution (DS) of 0.7. Tupa *et al.* (2015) used α -hydroxycarboxylic acid as catalyst and successfully produced starch acetate with DS of 0.03-2.93 at temperature of 90-140 °C. Using acid as catalyst has limitation especially during recovering of starch ester. Large amount of water may be needed to wash off the acid catalyst as well as the acylant acid anhydride. Termination of an esterification process usually involves addition of water. Addition of water may convert acid anhydride into acid form. Thus, a large volume of water is needed to wash off the acid from acid anhydride and acid catalyst. In contrast, utilisation of sodium hydroxide as catalyst may partially neutralise the

acid from acid anhydride during addition of water. This makes the recovery of starch ester easier (El Halal *et al.*, 2015). Starch acetates with different degrees of substitution were produced using different concentrations of sodium hydroxide; 11% NaOH (DS 0.08); 17% NaOH (DS 0.22); 23% NaOH (DS 0.31) at reaction temperature of 100 °C. Pyridine was also used as catalyst during the preparation of starch ester. At 80-105 °C, OSA starch with DS of 0.57-1.21 was produced in the presence of pyridine. However, the toxicity of pyridine could pose environmental pollution (Bourget *et al.*, 2014). More environmentally friendly catalyst used recently was from ionic liquid and enzyme. Zarski *et al.* (2016) produced starch oleate with DS of 0.09-0.22 using ionic liquid and enzyme immobilised lipase at 60-80 °C. The high cost of these catalysts was the main drawback.

2.10 Applications of starch ester

When starch acetate was used to prepare pudding, it exhibited better sensorial properties (external thickness, cohesiveness, melting and smoothness) than native starch pudding (Sun *et al.*, 2016). Muffin incorporated with OSA starch as partial fat replacement, had higher specific volume and softer texture compared with muffin added with maltodextrin. Muffin prepared with OSA starch (produced under acidic conditions) tended to have a greater volume, probably due to its lower molecular weight. OSA starch prepared at pH 6, when used to prepare muffin, contributed to the softness of muffin which resembled the texture of full-fat muffin (Chung *et al.*, 2010).

The health benefit of starch acetate has also been studied. Starch acetate was incorporated into rat's diet containing cholesterol. Rats fed with starch acetate diet

had the same body weight gain as those fed with control diet (cellulose). Rats fed with starch acetate diet had significantly lower pH of caecal content, lower pH of colonic content and produced lower ammonia in digesta compared to those fed with control diet (Wronkowska *et al.*, 2011). Microflora hardly fermented starch acetate into putrefactive compounds such as ammonia but instead utilised starch acetate as an additional source of energy (He *et al.*, 2017). Starch acetate diet was fermented into acetic acid (307.2 $\mu\text{mol}/100$ g body weight); propionic acid (96.72 $\mu\text{mol}/100$ g body weight) and butyric acid (25.61 $\mu\text{mol}/100$ g body weight). On the other hand, control diet (cellulose) was fermented into acetic acid (63.2 $\mu\text{mol}/100$ g body weight), propionic acid (12.10 $\mu\text{mol}/100$ g body weight) and butyric acid (7.85 $\mu\text{mol}/100$ g body weight). The liberated short chain fatty acids by microflora could be absorbed and used by colonocytes and gut microflora. Lowering of colonic pH tends to encourage the growth of healthy bacteria and reduced the growth of pathogenic bacteria in the colon (Arcila & Rose, 2015; Haenen *et al.*, 2013), thus improving bowel health. Caecal bacterial enzyme activity in rats fed with starch acetate diet had a significantly reduced beta-glucuronidase enzyme activity compared to control diet. The low activity of this enzyme is important because beta-glucuronidase activity is related to the formation of toxic and carcinogenic metabolites in the hindgut (Shi *et al.*, 2016b). Starch acetate diet also assisted in the reduction of serum total cholesterol and triglyceride compared to control diet (Wronkowska *et al.*, 2011). The reduction of serum total cholesterol was due to fecal excretion of sterols and inhibition of cholesterol production through short chain fatty acids. The reduction of triacylglyceride was attributed to the decrease in hepatic fatty acid synthesis (Verbeke *et al.*, 2015).

Starch acetate (DS 1.9 or 2.6) in the form of microparticles and films were used to deliver timolol, calcein or BSA. Starch acetate microparticles exhibited continuous sustained release of timolol and calcein. Starch acetate (DS 2.6) film incorporated with calcein and BSA displayed discontinuities in drug release profile, implying that their release was erosion-controlled. Enzyme α -amylase was also added to starch acetate film to increase the release of drug. The addition of enzyme α -amylase promoted film erosion and increased the initial fast release of BSA from starch acetate (DS 1.9) film. Influence of α -amylase on the film prepared with starch acetate (DS 2.6) was modest. The low hydrolysis of starch acetate (DS 2.6) was due to the steric hindrance of ester group that could not fit into the enzyme's active site. Starch acetate microparticles and film could be used to prepare slow release formulations of different molecular weight of drugs compared to native starch that contributed to fast release of drugs (Tuovinen *et al.*, 2004a). In another study, starch acetate microparticles containing calcein were prepared with water-in-oil-in-water double emulsion technique. The starch acetate microparticles were added to cultured human retinal pigment epithelium (RPE) cell line (D407) and examined for their cellular uptake and degradation. During the incubation in RPE-cell culture, the absorption of starch acetate microparticles was reported as 8.1%. Enzyme within the RPE cells could degrade the starch acetate microparticles within the cells. This starch acetate had slower degradation and swelling than native starch. Starch acetate microparticles had the potential to deliver drug to the RPE for ocular treatment (Tuovinen *et al.*, 2004b).

Corn starch ester is one of the ingredients used to produce eye cream containing active ingredients such as live yeast cell derivative, magnesium ascorbyl phosphate,